Identifying Mangrove Species and Their Surrounding Land Use and Land Cover Classes Using an Object-Oriented Approach with a Lacunarity Spatial Measure

Soe W. Myint[1]
School of Geographical Sciences, Arizona State University, P.O. Box 870104, Tempe, Arizona 85287-0104

Chandra P. Giri
Science Applications International Corporation (SAIC)/U.S. Geological Survey, Center for Earth Resources Observation and Science (EROS), Sioux Falls, South Dakota 57198-0001

Le Wang
Department of Geography, University at Buffalo, State University of New York, 105 Wilkeson Quadrangle, Buffalo, New York 14261

Zhiliang Zhu
U.S. Geological Survey, Center for Earth Resources Observation and Science (EROS), Sioux Falls, South Dakota 57198-0001

Shana C. Gillette
Institute for Animal Population Health, and Department of Journalism and Technical Communication, Colorado State University, Ft. Collins, Colorado 80523

Abstract: Accurate and reliable information on the spatial distribution of mangrove species is needed for a wide variety of applications, including sustainable management of mangrove forests, conservation and reserve planning, ecological and biogeographical studies, and invasive species management. Remotely sensed data have been used for such purposes with mixed results. Our study employed an object-oriented approach with the use of a lacunarity technique to identify different mangrove species and their surrounding land use and land cover classes in a tsunami-affected area of Thailand using Landsat satellite data. Our results showed that the object-oriented approach with lacunarity-transformed bands is more accurate (overall accuracy 94.2%; kappa coefficient = 0.91) than traditional per-pixel classifiers (overall accuracy 62.8%; and kappa coefficient = 0.57).

[1]Email: soe.myint@asu.edu

GIScience & Remote Sensing, 2008, **45**, No. 2, p. 188–208. DOI: 10.2747/1548-1603.45.2.188

INTRODUCTION

Mangrove forests, found in intertidal zones in the tropics and subtropics, are among the most productive ecosystems of the world. The forests often form conspicuous zones or bands of species. The zonation is associated with a number of external factors, including tidal inundation, land elevation, seedling dispersal, and soil condition with regard to nutrient availability, oxygen deficiently, and salinity, but the dominating factor may vary in different parts of the world. There are six categories of hypotheses to explain the zonation: (1) land building and plant succession (Davis, 1940); (2) geomorphological influences (Thom, 1967); (3) physio-chemical gradients and zonation; (4) propagule dispersal and zonation (Rabinowitz, 1978), (5) propagule predation and forest structure (Smith, 1987; McKee, 1995), and (6) competition and forest structure (Ball, 1980).

The complex nature of mangroves' root systems recycles nutrients and traps debris as well as suspends sediments and solids that are brought to the coast by streams and rivers. The forests and their complex root systems also provide prevention against shoreline erosion. Different kinds of mangrove species function as an irreplaceable aquatic ecosystem for feeding and serving as nursery grounds for many ecologically and economically valuable living aquatic resources and organisms, including oysters, algae, barnacles, sponges, fish, shellfish, prawns, and crabs. Mangrove forests also function as an important habitat for the health of near-shore ecosystems such as seagrass beds and coral reefs. Wang et al. (2004b) reported that the spatial arrangements of component species in mangrove forests are often differentially distributed with distance from the water's edge. They usually form zones of differing mangrove species compositions vertical to the intertidal rise.

As stated earlier, there are significant economic and ecological values in mangrove habitats. The mangrove forests, however, are declining at an alarming rate—perhaps even more rapidly than inland tropical forests (Aizpuru et. al., 2000). Many of the remaining mangrove forests are degraded (UNEP, 2004) and under immense pressure from clearcutting, hydrological alterations, chemical spills, and climate changes (Aschbacher et al., 1994; Giri and Delsol, 1995, Blasco et al., 2001; Giri et al., 2007). At the same time, their health and persistence are seriously threatened by urban growth, infrastructure development, fuel-wood consumption, and development of aquatic farming systems. Campenhout (1997) reported that the disappearance of a type of species in a mangrove forest could be the initial process of a chain reaction that leads to the inability of the ecosystem to fulfill its vital role against coastal erosion that threatens human settlements and coastal plantations. The disappearance of a mangrove species may also have an impact on the associated ecosystems such as seagrass beds and coral reefs that will be affected by the sedimentation process of suspended material displaced from the mangroves. Hence, it has been suggested that the study of mangrove dynamics, both spatially and temporally in terms of density, crown closure, species richness, growth, deforestation, and regeneration capacity, are considered very important (Dahdouh-Guebas et al., 2000).

There is an emerging need to assess mangrove forest structure and dynamics to gain a better understanding of their ecosystems and make a better management plan for sound conservation and restoration efforts. Hence, the ability to identify mangrove species with the use of remote sensing and geospatial information could play an important role in implementing this important task. Accurate and reliable information on the spatial distribution of mangrove species is needed for a wide variety of applications, including sustainable management of mangrove forests, conservation and reserve planning, ecological and biogeographical studies, and invasive species management. Traditional methods for mapping species distribution involve intensive, time consuming, and costly field works. Remotely sensed data such as Landsat and SPOT have been used for such purposes with mixed results (Wang et al., 2004a). Aschbacher et al. (1995) and Ravan and Roy (1997) used NDVI values to separate vegetative areas from barren areas and to assess mangrove distributions. However, the coarse resolutions of these data sources do not allow identification at the species level within a mangrove forest (Holmgren and Thuresson, 1998).

Wang et al (2004b) reported that remotely sensed images have not been used widely for mapping mangrove species because of the limited spectral and spatial resolution of conventional imageries. It was also pointed out that spatial resolution plays a more important role than spectral resolution in discriminating different mangrove species. Green et al. (1998) demonstrated that accurate discrimination among mangrove species was not possible with conventional satellite data, but was possible using images from an airborne sensor such as CASI. Jusoff (2006) used airborne hyperspectral imaging data to map individual mangrove species in Port Klang, Malaysia and reported that the individual species could only be identified at the near infrared portion of the electromagnetic spectrum and not in the visible spectrum. However, the study did not provide the classification accuracy or the possibility of discriminating different mangrove species. Moreover, from the spectral profiles of nine mangrove species provided in the manuscript, we cannot make a firm conclusion that the spectrum of all nine mangrove species were significantly different. Wang et al. (2004b) tested different combinations of spectral and textural information inherited in IKONOS and QuickBird satellite data for classifying three mangrove species on the Caribbean Coast of Panama. Results indicated that IKONOS performed slightly better than QuickBird. Held et al. (2003) achieved a satisfying accuracy when integrating the high–spatial/spectral–resolution scanner CASI and the airborne AIRSAR. Wang and Sousa (2007) conducted a laboratory analysis of mangrove leaf spectral reflectance collected with a spectrometer. Results revealed that mangrove species can be well discriminated at leaf level in the lab condition.

From the above discussion, it is apparent that the identification of different mangrove species using conventional median-resolution remote sensor data (e.g., Landsat TM, ASTER, SPOT) remains a challenging task. The main goal of the present study is to map species distribution of mangrove forests using Landsat satellite data and object-oriented classification approach. The study aims to employ an object-oriented approach with the use of a lacunarity technique introduced by Myint and Lam (2005a) to identify different mangrove species and their surrounding coastal land use and land cover classes in a tsunami-affected area of Thailand using a Landsat TM image data. We anticipated that lacunarity (Mandelbrot, 1995), which is capable of discriminating different spatial features that may share the same fractal dimension values, may augment the object-oriented approach by accurately identifying mangrove species and other land use and land cover classes in the study area.

Fig. 1. Map of study area.

DATA AND STUDY AREA

Landsat Thematic Mapper image data (path 37 and row 37) at 28.5 m spatial resolution with seven channels ranging from blue to the thermal infrared portion of the spectrum was used in this study. The image data were acquired over an area with three different types of mangroves in Trang Province, Thailand on January 9, 1991. The location of the study area on the Andaman Sea coast is presented in Figure 1. The original image was subset to extract the study area (upper left longitude 99° 19' 0.54" and latitude 7° 29' 57.52", lower right longitude 99° 40' 05.92" and latitude 7° 08' 07.97") that covers approximately 1,558 km^2 (1359 × 1411 pixels). The study area contains common land use and land cover classes in a coastal area: mangroves, built-up, bare soil, woodlands and other vegetation cover, ocean, river, lakes, ponds, sandbars, and exposed soil (Fig. 2).

Mangrove forests in the Andaman Sea coast of Thailand can be categorized into five major groups of mangroves depending on the dominant species associated with the groups: *Rhizophora*, *Nypa*, *Malaleuca*, *Avicennia*, and peat forest. *Rhizophora* is the most commonly found group in the Andaman sea coast and covers about 80 percent of the total mangrove area (IUCN, 2006). The mangrove forest types we attempted to identify in the study area include *Rhyzophora*, *Malaleuca*, and *Nypa*. The most commonly found mangrove species in the *Rhizophora* group include *Rhizophora apiculata* and *Rhizophora mucronata*. *Nypa fruitican* and *Malaleuca cajuputi*

Fig. 2. False-color composite of the study area displaying channel 4 (0.76–0.90 μm) in red, channel 3 (0.63–0.69 μm) in green, and channel 2 (0.52–0.60 μm) in blue.

are the dominant species of *Nypa* and *Malaleuca* groups, respectively. We consider oceans, rivers, lakes, and ponds together as a water class. In addition to the classes described above, we also identified clouds and cloud shadows.

A mangrove species composition map of tsunami-hit areas in Thailand prepared by the World Conservation Union (IUCN) in collaboration with Department of Marine and Coastal Resources (IUCN, 2006) was used to select training samples of the mangrove forest types and to assess the classification accuracy of output maps (Fig. 3). The hard-copy map only shows the three mangrove forest types, and was prepared through the manual delineation of individual species with the help of an extensive forest inventory. The IUCN research team conducted GPS-guided field investigations in October and November of 2005 to validate the classification outputs. The team conducted field work along 40 GPS coded transects totaling 850 km in length and 189 GPS points in the coastal districts and regions that represent four major mangrove forest groups. They documented locations of the ground truth transects and points within the provinces. The existing mangrove classification map previously prepared by the Royal Forest Department was also used to cross validate the IUCN's classification results during the field observations. Even though the classification accuracy assessment reports for 21 mangrove species distribution maps

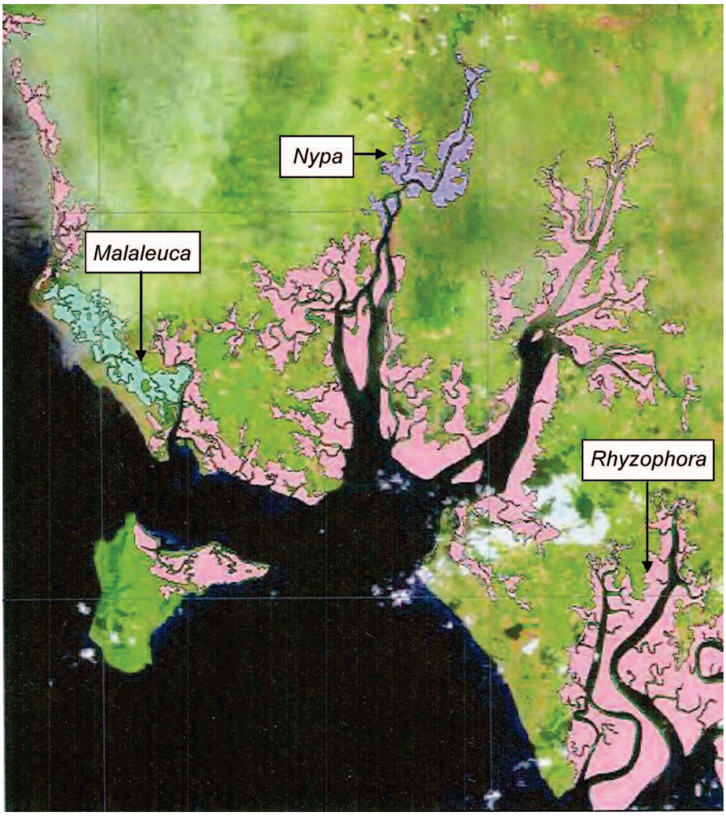

Fig. 3. Reference map (IUCN, 2006).

were not available in IUCN (2006), the technical report clearly stated that the classification accuracy of the outputs was superior. This could have been due to the fact that the manual digitization was carefully carried out with the help of sound local area knowledge, a careful comparison with existing mangrove forest maps prepared by the Royal Forest Department, and a thorough ground survey for interpretation. Hence, the classification output generated from the manual interpretation is assumed to be highly accurate with a negligible error. Training sample selection and validation of the classification accuracy was also supplemented by local-area knowledge of the research team and field work recently conducted in tsunami-hit mangrove areas of Thailand.

OBJECT-ORIENTED APPROACH

The method employed here for identifying different mangrove forest types and their surrounding land use and land cover classes in Landsat Thematic Mapper data included five steps that employed five levels of scale: (1) scale level 1—segmentation of water bodies using a blue ratio band with a rule-based approach; (2) scale level 2—classification of cloud shadows using a multispectral band combination of channels, 1, 2, 3, 4, 5, 6, and 7 at a scale lower than the scale employed in the first step; (3) scale level 3—identification of clouds using a combination of bands 1, 2, and 7 at a scale coarser than the second step; (4) scale level 4—classification of general land use and land cover classes such as built-up, bare soil, sand, mangroves, and other forest types using a combination of multispectral bands and lacunarity-transformed bands 3, 4, and 5 at a scale lower than the previous step; and (5) scale level 5—discrimination of three different mangrove forest types using the same combination as described above at a coarser scale. This study employed a greyscale lacunarity approach introduced in Myint and Lam (2005a) for generating lacunarity-transformed bands for effectively discriminating different mangrove species. It was anticipated that the identification of mangrove species in 28.5 m resolution Landsat TM with the original spectral bands alone are practically not viable because they are spectrally similar.

Lacunarity

Mandelbrot (1983) introduced the term lacunarity (*lacunar* is Latin for “gap”) to characterize different texture appearances that may have the same fractal dimension value. It was reported that fractal dimensions may be far from providing a complete characterization of a set’s texture. In other words, different fractal sets may share the same fractal dimension values but show different spatial appearances (Mandelbrot, 1983; Voss, 1986; Dong, 2000; Myint, et al., 2006). Mandelbrot (1995) stated that different fractal sets that share the same dimension value may be constructed, but may look completely different because they have different lacunarity. Since lacunarity represents the distribution of gap sizes, low-lacunarity objects are homogeneous because all gap sizes are the same, whereas high-lacunarity objects are heterogeneous (Dong, 2000).

As an initial step toward quantifying texture or spatial arrangements of objects and features effectively, Voss (1986) proposed a probability approach to estimate the fractal dimension and lacunarity of image intensity surface. Myint and Lam (2005a) reported the development of a lacunarity algorithm introduced in mathematical terms by Voss (1986) and provided an initial exploration of the lacunarity approach in comparison to fractal and spatial autocorrelation approaches. It was found that lacunarity was the most accurate, and lacunarity-transformed images improved the classification accuracy dramatically (Myint and Lam, 2005b). Hence, this study employs a lacunarity approach reported in Myint and Lam (2005a) to effectively map different mangrove species and their surrounding land use and land cover.

I provide a brief description of the approach below (see Myint and Lam, 2005a for details). The spatial arrangement of the points determines $P(m,L)$. $P(m,L)$ is the probability that there are m intensity points within a box size of L centered about an arbitrary point in an image. Intensity points are referred to as the number of points that fill in a cube box. Hence, we have

$$\sum_{m=1}^{N} P(m,L) = 1 \tag{1}$$

where N is the number of possible points in the box of L. Suppose that the total number of points in the image is M. If one overlays the image with boxes of side L, then the number of boxes with m points inside the box is $(M/m)P(m,L)$. Hence

$$M(L) = \sum_{m=1}^{N} mP(m,L) \tag{2}$$

and

$$M^2(L) = \sum_{m=1}^{N} m^2 P(m,L). \tag{3}$$

Lacunarity can be computed from the same probability distribution $P(m,L)$. Hence, lacunarity is defined as

$$\Lambda(L) = \frac{M^2(L) - (M(L))^2}{(M(L))^2} \tag{4}$$

A worked example for computing a lacunarity value is also presented in Myint and Lam (2005a).

Lacunarity represents the distribution of gap sizes: low lacunarity features are homogeneous because all gap sizes are the same, whereas high lacunarity features are heterogeneous (Myint et al., 2006). Texture-transformed images of band 3, band 4, and band 5 derived from the lacunarity approach were employed in identifying general land use and land cover classes and the three mangrove species. We used 5 × 5 local window to compute lacunarity values. The computed lacunarity value is assigned to the center of a local window and the window moves throughout the image. Since computed lacunarity values are floating point numbers, we converted lacunarity-transformed bands to unsigned 8 bit data using a standard deviation stretch. The lacunarity bands will be hereafter called V5, V4, and V3. An example texture-transformed image of Landsat TM data (i.e., band 5) is shown in Figure 4.

Image Segmentation

Regarding the object-oriented approach in image classification, a group of pixels having similar spectral and spatial properties is considered an object. Hence, an object-based classification approach employs segmented objects at different scale levels as fundamental units for image analysis instead of utilizing a per-pixel approach at a single scale for classification (Navulur, 2007; Desclée et al., 2006).

Image segmentation is a principal function that splits an image into separate regions or objects depending on parameters specified. We used eCognition professional 4.0 to perform an object-based classification. The segmentation function in eCognition software (Baatz and Shape, 1999, 2000) is based on three parameters, namely shape (S_{sh}), compactness (S_{cm}), and scale (S_{sc}) parameters. Users can apply

Fig. 4. A lacunarity-transformed image of Landsat TM band 5.

weights ranging from 0 to 1 for the shape and compactness factors to determine objects at different level of scales. These two parameters control the homogeneity of different objects. The shape factor adjusts spectral homogeneity vs. shape of objects, whereas the compactness factor, balancing compactness and smoothness, determines the object shape between smooth boundaries and compact edges. The scale parameter that controls the object size that matches the user's required level of detail can be considered the most crucial parameter of image segmentation. Different levels of object size can be determined by applying different numbers in the scale function. The higher scale number (e.g., 100) generates larger homogeneous objects (smaller scale—lower level of detail), whereas a smaller scale number (e.g., 10) will lead to smaller objects (larger scale). A smaller number used in the scale parameter corresponds with a higher level in the segmentation procedure. The decision on the scale level depends on the size of the object required to achieve the goal. The software also allows users to assign different levels of weighting to different bands in the selected image during image segmentation.

Image Classification

Regarding selection of objects to assign classes, there are two options to control. The membership function defines rules and constraints to control the classification procedure based on the user's expert knowledge. The nearest neighbor option is a non-parametric classifier and is therefore independent of the assumption that data values follow a normal distribution. This technique allows unlimited applicability of the classification system to other areas, requiring only the additional selection or modification of new objects (training samples) until a satisfactory result is obtained (Ivits and Koch, 2002). Application of the nearest neighbor method is also advantageous when classes are spectrally similar and not well separated using a few features or just one feature (Definiens, 2004). The nearest neighbor approach in eCognition can be applied to any class at any level using any original, composite, transformed, or customized bands. There are two options available with the nearest neighbor function, namely (1) Standard Nearest Neighbor, and (2) Nearest Neighbor. The Standard Nearest Neighbor option automatically selects the mean values of objects for all the original bands in the selected image, whereas the second option requires users to identify variables (e.g., shape, texture, hierarchy) under object features, class-related features, or global features. The steps employed in this study to map different mangrove forest types and their associated land use and land cover classes at each scale level are described below.

Level 1. We identified water pixels using a rule-based classification approach at the highest level of scale. The shape parameter (S_{sh}) was set at 0.1 to give less weight to shape and give more attention to spectrally more homogeneous pixels for image segmentation. The compactness parameter (S_{cm}) was set at 0.5 to balance compactness and smoothness of objects equally. We used the above shape and compactness parameters for all steps and levels. To obtain the finest objects possible, including small tributaries and ponds, the scale parameter (S_{sc}) was set to 1. This is basically a pixel-level scale. We attempted several original, composite, ratio, and customized bands and found that blue-ratio band was the most effective band in accurately identifying water bodies. The blue-ratio band in eCognition is defined as the blue band divided by the summation of all other bands, and contains digital numbers (DN) between 0 and 1. For this image, water values range from 0.31 to 1. To create a rule-based approach, we selected a function that encompasses all the DN values between 0.31 and 1, including either value. We classified water bodies using the above expert-system rule and saved them as a water layer.

Level 2. We attempted to identify cloud shadows using all Landsat TM bands, including the thermal band. The scale parameter (S_{sc}) was set to 5 for the segmentation of cloud shadows. We identified five to seven training samples of cloud shadows, and several samples of other classes including clouds, water, and other. We included a thermal band to separate shadow pixels and dark water pixels. The nearest neighbor classifier was used to identify the classes. We identified different samples iteratively and classified cloud shadows until we received satisfactory results. Even though we identified cloud, water, and other classes, we discarded these classes and used only cloud shadows.

Level 3. The scale parameter (S_{sc}) was set to 10 for segmenting objects at this level. We identified about five objects of clouds as training samples for clouds after segmenting the selected image. We used only bands 1, 2, and 7 of a Landsat TM image for cloud identification. We tried several band combinations and found that the above three bands were the best combination to achieve a satisfactory result for clouds. We also selected some object samples for other classes such as water and cloud shadows. Cloud pixels identified at this scale level were the only pixels retained for the final map.

Level 4. We used a combination of Landsat TM bands 1, 2, 3, 4, 5, 7 and lacunarity-transformed bands of Landsat TM bands 3, 4, and 5 for land use and land cover classification at this level. We used the scale parameter of 25 to segment objects. We selected training objects for bare soil, built-up, mangroves, other forest, sand, and water. We also employed the nearest neighbor classifier. We did not keep mangroves and water for the final map preparation since the accurate water bodies were identified at level 1 and detailed mangrove forest types were identified at level 5 (lowest level).

Level 5. We also used the same band combinations above, including lacunarity-transformed bands 3, 4, and 5. The scale parameter (S_{sc}) was set to 50 for the segmentation of the three mangrove species (i.e., *Nypa*, *Malaleuca*, and *Rhyzophora*). We selected four to five training objects per species to perform the nearest neighbor classification approach.

We overlaid layers at different levels to produce a final output map of mangrove types and their surrounding land use and land cover. The first GIS overlay function started with the last two layers and extracted the three mangrove species, bare soil, built-up, mangroves, other forests, and sand. This output map was overlaid on the map produced at level 4 to add cloud pixels. We later obtained cloud shadows and water bodies from the last two layers generated at scale levels 2 and 1. A small subset of the study area shows segmented objects at all levels except level 1 (pixel level) in Figure 5. A flow chart that demonstrates a step-by-step procedure to conduct this research study is presented in Figure 6. The output map of the object-oriented approach using lacunarity-transformed bands is shown in Figure 7.

PER-PIXEL CLASSIFIER

To evaluate the effectiveness of the object-oriented approach using lacunarity-transformed bands, we also employed the most commonly used supervised decision rule, namely the maximum likelihood classifier. The maximum likelihood decision rule is based on the probability that a pixel belongs to a particular class. The basic equation of the decision rule assumes that these probabilities are equal for all classes (Jensen, 2004; Lillesand et al., 2004). Traditional per-pixel classifiers use a combined spectral response from all training-set pixels for a given class. Hence, the resulting signature comprises responses from a group of different land covers in the training samples, and the classification system simply ignores the impact of mixed pixels (Lu and Weng, 2007).

The parametric decision rules are based on the assumption that data values follow a normal distribution, and that the statistical parameters (e.g. mean, variance, covariance matrix) generated from the training samples are representative. However, the assumption of a normal spectral distribution could potentially lead to some errors if the data is not normally distributed. We selected three to six training samples per class that are spectrally different for the classification. We also attempted several different sets of training samples and qualitatively evaluated the outputs. We merged those classes generated by different training samples under the same land use and land cover category. The resulting land use and land cover categories were the same as

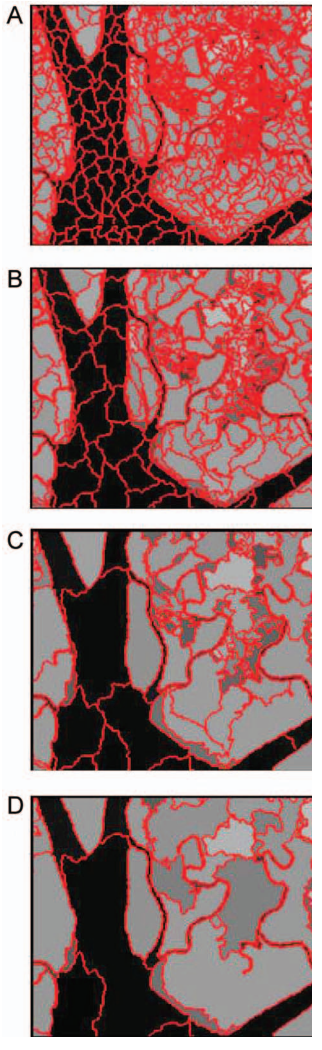

Fig. 5. Segmented objects at all levels except level 1. Scale level 1 is not included because it is similar to the original image (pixel level). A. Scale 5. B. Scale 10. C. Scale 25. D. Scale 50.

those identified with an object-oriented approach. We produced several outputs and selected the best output as the final map of the maximum likelihood classifier. The output map produced by the traditional classifier is presented in Figure 8.

ACCURACY ASSESSMENT

For the classification accuracy assessment, error matrices were produced and analyzed for each method. These error matrices show the contingency of the class to which each pixel truly belongs (columns) on the map unit to which it is allocated by the selected analysis (rows). From the error matrix, overall accuracy, producer's

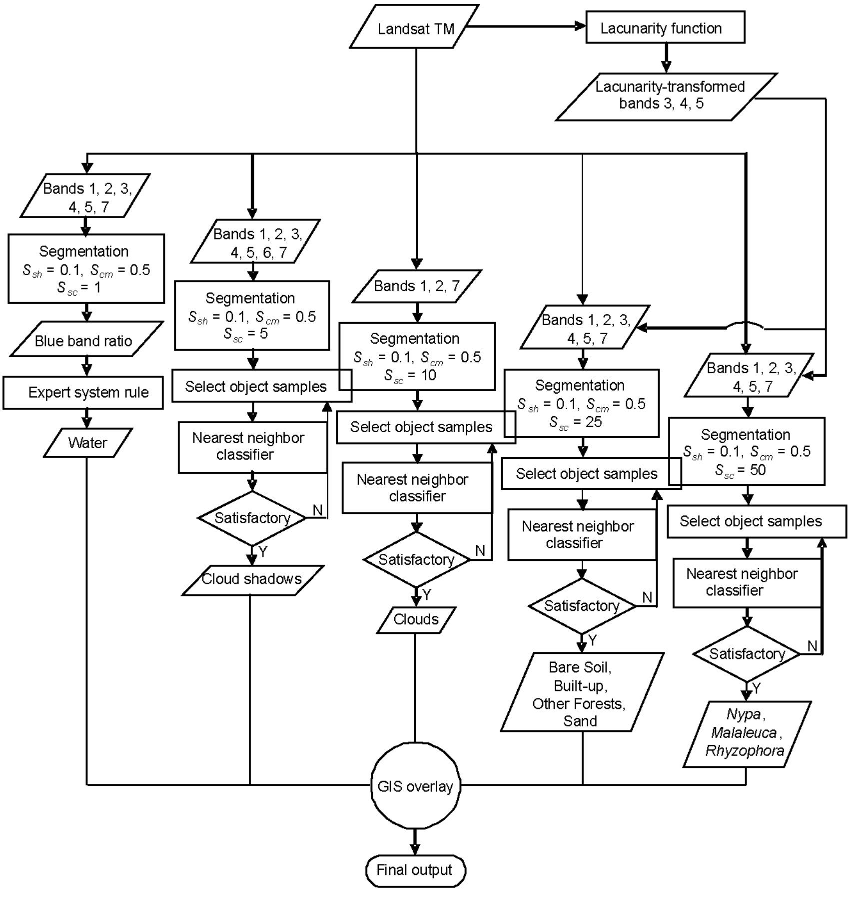

Fig. 6. Flow chart of the approach employed in the study.

accuracy, user's accuracy, and the kappa coefficient were generated. Congalton (1991) suggested that a minimum of 50 sample points for each land use/land cover category in the error matrix be collected for the accuracy assessment of any image classification. We selected 500 sample points that led to approximately 50 points per class (10 total classes) for the accuracy assessment. A minimum of 20 points per class was set for generating 500 points using a stratified random sampling approach. To be consistent and for precise comparison purposes, we used the same sample points for the outputs generated by the object-oriented classifier and the traditional classification technique (i.e., maximum likelihood). For a better evaluation, we performed the classification accuracy assessment on the original output maps. We did not edit, manually correct, or filter any of the two output maps.

RESULTS AND DISCUSSION

As mentioned earlier, we anticipated that the identification of mangrove species in 28.5 m resolution Landsat TM with the original spectral bands alone with the

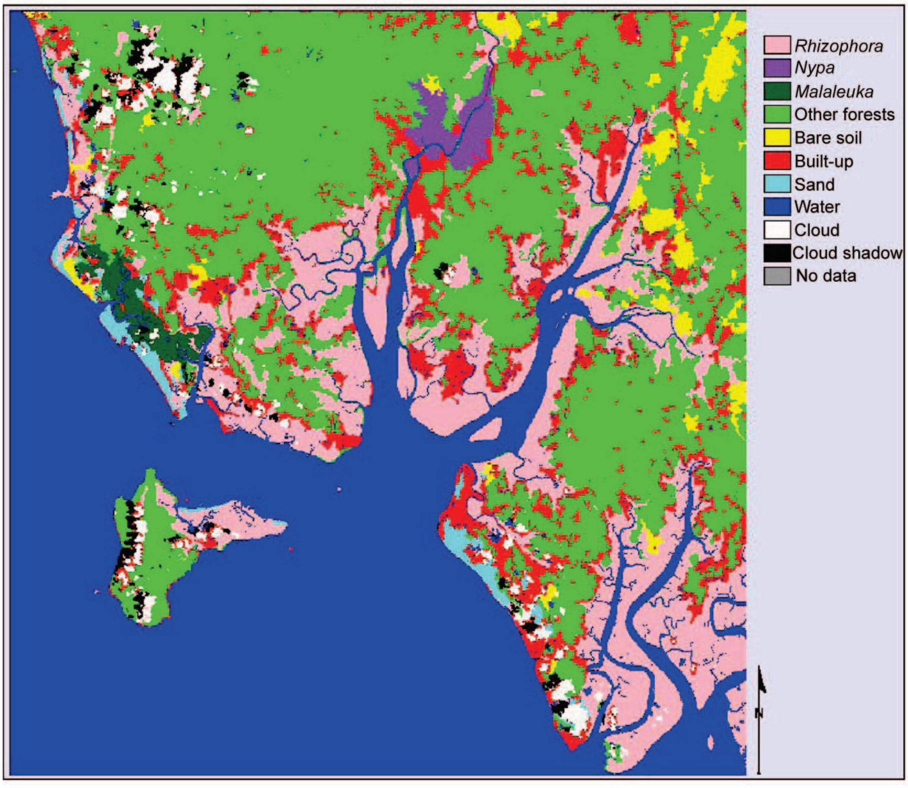

Fig. 7. Output map generated by the object-oriented approach using lacunarity-transformed bands. The output image was not manually edited or filtered.

traditional classifiers (i.e., maximum likelihood) may not be very effective because they are spectrally similar. By qualitative evaluation (visual examination on screen) of the output maps, we noticed that the output map generated by the traditional per-pixel approach contains many mistakenly identified pixels of classes (Fig. 8), whereas the output map generated by the object-oriented classifier with the lacunarity approach is more accurate and satisfactory (Fig. 7).

The traditional classification approach produced an overall accuracy of 62.8%, which is far below the minimum mapping accuracy of 85% required for most resource management applications (Anderson et al., 1976; Townshend, 1981). The kappa coefficient for this approach is 0.57. This can be thought of as an indication that an observed classification is only 57% better than one resulting from chance. From Table 1, it can be observed that the maximum likelihood rule gave the highest producer's accuracies for water and cloud shadows (100%). Even though water and cloud shadow pixels have been correctly identified, only 92% (water) and 59% (cloud shadow) of the areas identified as water and cloud shadow within the classification are truly of the respective categories. The water category also gave the highest user's accuracy (92%). The lowest user's accuracy was given by bare soil. As expected

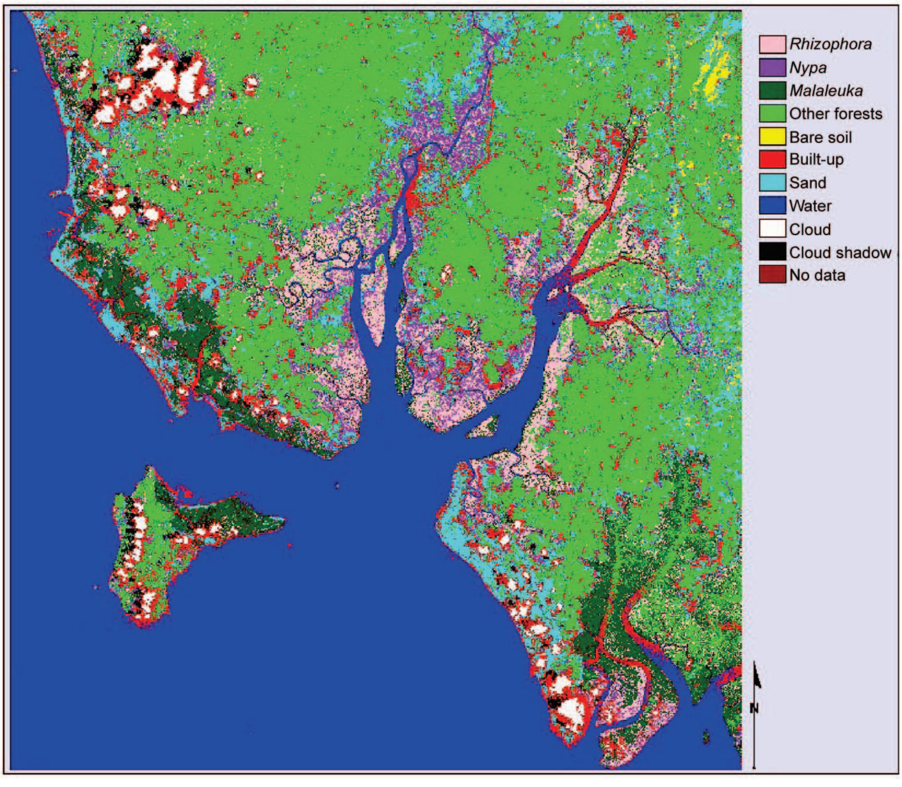

Fig. 8. Output map generated by the traditional per-pixel classification approach (i.e., maximum likelihood). The output image was not manually edited or filtered.

earlier, user's and producer's accuracies for the mangrove species *Rhyzophora*, *Nypa*, and *Malaleuka* were very low.

In contrast to the traditional approach, the object-oriented approach yielded an overall accuracy far above the minimum overall accuracy (85%) required for most applications (94.2%). It can be observed from Table 2 that an observed classification for this approach is 93% (kappa) better than one resulting from chance. The lowest producer's accuracy was given by built-up (81%) and the lowest user's accuracy was given by other forests (82%). There is some signature confusion between built-up vs. other forest and sand vs. other forests categories. Some pixels identified as other forests were found to be bare soil, built-up, and sand categories on the ground. The three mangrove species (i.e., *Rhyzophora*, *Malaleuca*, *Nypa*) produced very high producer's and user's accuracies. The lowest producer's and user's accuracies for the three mangrove species produced by the object-oriented approach were 91% and 96%, respectively, whereas the same accuracies for the same species generated by the per-pixel approach were 51% and 29%. This confirms that the object-oriented approach with lacunarity-transformed bands outperforms the traditional classification approach. This was partly because there are many features and variables as well as

Table 1. Overall Accuracy, Producer's Accuracy, User's Accuracy, and Kappa Coefficient Produced by the Per-pixel Classifier (i.e., maximum likelihood)[a]

Classified	Reference										Total	Pr-Ac, pct.	Ur-Ac, pct.
	Rh	Ny	Ma	Of	So	Bu	Sa	Wa	Cl	Sh			
Rh	17	5	3	3	0	0	0	0	0	0	28	61	29
Ny	4	21	2	2	4	0	2	0	0	0	35	60	70
Ma	19	0	23	1	0	0	0	1	1	0	45	51	70
Of	9	2	2	76	8	4	1	5	0	4	111	68	66
So	1	0	0	0	8	0	0	0	0	0	9	89	26
Bu	5	0	2	16	0	12	4	2	17	5	63	19	44
Sa	4	2	1	18	11	10	21	0	1	3	71	30	72
Wa	0	0	0	0	0	0	0	98	0	0	98	100	92
Cl	0	0	0	0	0	1	1	0	21	0	23	91	53
Sh	0	0	0	0	0	0	0	0	0	17	17	100	59
Total	59	30	33	116	31	27	29	106	40	29	500		

[a]Rh = *Rhyzophora*; Ny = *Nypa*; Ma = *Malaleuca*; Of = Other forests; So = Bare soil; Bu = Built-up; Sa = Sand; Wa = Water; Cl = Clouds; Sh = Cloud shadows; Pr-Ac = Producer's accuracy; Ur-Ac = User's accuracy. Overall accuracy = 62.80%; kappa coefficient = 0.57.

Table 2. Overall Accuracy, Producer's Accuracy, User's Accuracy, and Kappa Coefficient Produced by the Object-Oriented Approach with Lacunarity-Transformed Bands[a]

	Reference												
Classified	Rh	Ny	Ma	Of	So	Bu	Sa	Wa	Cl	Sh	Total	Pr-Ac, pct.	Ur-Ac, pct.
Rh	53	0	0	5	0	0	0	0	0	0	58	91	96
Ny	0	33	0	0	1	0	0	0	0	0	34	97	100
Ma	0	0	34	0	0	0	0	0	0	0	34	100	100
Of	2	0	0	84	0	1	0	0	0	0	87	97	82
So	0	0	0	4	31	0	1	0	0	0	36	86	97
Bu	0	0	0	6	0	38	0	0	2	1	47	81	97
Sa	0	0	0	4	0	0	29	0	1	0	34	85	97
Wa	0	0	0	0	0	0	0	101	0	0	101	100	99
Cl	0	0	0	0	0	0	0	0	35	0	35	100	92
Sh	0	0	0	0	0	0	0	1	0	33	34	97	97
Total	55	33	34	103	32	39	30	102	38	34	500		

[a]Rh = *Rhyzophora*; Ny = *Nypa*; Ma = *Malaleuca*; Of = Other forests; So = Bare soil; Bu = Built-up; Sa = Sand; Wa = Water; Cl = Clouds; Sh = Cloud shadows; Pr-Ac = Producer's accuracy; Ur-Ac = User's accuracy. Overall accuracy = 94.20%; kappa coefficient = 0.93.

many functions available with eCognition software that provided tremendous opportunities to improve classification accuracy.

CONCLUSION

We employed an object-oriented approach using lacunarity-transformed bands in comparison with a commonly used classifier (i.e., maximum likelihood) to identify the three mangrove species and their surrounding land use and land cover classes in a coastal area. Traditional per-pixel approaches (e.g., maximum likelihood classifier) were not effective in extracting coastal land use and land cover classes, especially species-level information of different mangrove forest types. It can be concluded that the object-oriented approach with lacunarity-transformed bands is more accurate than the traditional per-pixel classifiers. We believe the spatial information obtained from a lacunarity approach plays an important role in extracting mangrove species using the object-oriented approach. One of the main advantages of the object-oriented approach is that it allows additional rapid selection or modification of new objects (training samples) each time after performing a nearest neighbor classification until the satisfactory result is obtained. There are many possible combinations of different functions, parameters, features, and variables available with the software. However, it should be noted that the exact computation and operation of many of the parameters and functions available with eCognition software are not explicit. The successful use of eCognition largely relies on repeatedly modifying training objects, performing the classification, observing the output, and testing different combinations of functions as a trial-and-error approach. The availability of many different combinations of parameters, functions, features, and variables helped us identify land use and land cover classes and the three mangrove species effectively. Nonetheless, we would like to conclude that the object-oriented approach is effective and reliable in identifying detailed land use and land cover classes.

ACKNOWLEDGMENTS

This research has been supported by the National Science Foundation (grant # BCS-0649413) and Science Applications International Corporation (SAIC) under U.S. Geological Survey (USGS) contract # 03-CR-CN-0001.

REFERENCES

Aizpuru, M., Achard, F., and F. Blasco, 2000, "Global Assessment of Cover Change of the Mangrove Forests Using Satellite Imagery at Medium to High Resolution," in *EEC Research Project n 15017-1999-05 FIED ISP FR*, Ispra, Italy: Joint Research Centre.

Anderson, J., Hardy, E. E., Roach, J. T., and R. E. Witmer, 1976, *A Land Use and Land Cover Classification System for Use with Remote Sensor Data*, Sioux Falls, SD: USGS Professional Paper 964.

Aschbacher, A., Giri, C., Ofren, R., Tiangco, P. N., Suselo, T. B., Vibulsresth, S., and T. Charrupat, 1994, *Tropical Mangrove Vegetation Mapping Using Advanced Remote Sensing and GIS Technology (Executive Summary)*," Bangkok, Thailand:

Asian Institute of Technology, National Research Council of Thailand, Royal Forest Department, and UNEP-GRID.

Aschbacher, J. K., Ofren, R. B., Delsol, J. P., Suselo, T. B., Vibulsresth, S. K. and T. K. Charrupat, 1995, "An Integrated Comparative Approach to Mangrove Vegetation Mapping Using Advanced Remote Sensing and GIS Technologies; Preliminary Results," *Hydrobiologia*, 295:285-294.

Baatz, M. and A. Schape, 1999, "Object-Oriented and Multi-Scale Image Analysis in Semantic Networks," in Proceedings of the 2nd International Symposium on Operationalization of Remote Sensing, Enschede, Netherlands, ITC, August 16–20, 1999.

Baatz, M. And Schape, A., 2000, "Multiresolution Segmentation: An Optimization Approach for High Quality Multi-scale Image Segmentation," in *Proceedings of the Angewandte Geographische Informationsverarbeitung XII*, Strobl, J. et al. (Eds.), Salzburg, Austria: Beiträge zum AGITSymposium 2000, 12–23.

Ball, M. C., 1980, "Patterns of Secondary Succession in a Mangrove Forest in Southern Florida," *Oceologica* (Berlin), 44:226–235.

Blasco, F., Aizpuru, M., and C. Gers, 2001, "Depletion of the Mangroves of Continental Asia," *Wetlands Ecology and Management*, 9:245–256.

Campenhout, V., 1997, "High Spatial Resolution Remote Sensing of Forest Trees," *Journal of Trees*, 13(8):300–310.

Congalton, R. G., 1991, "A Review of Assessing the Accuracy of Classifications of Remotely Sensed Data," *Remote Sensing of Environment*, 37:35–46.

Dahdouh-Guebas, F., Verheyden, A. A., De Genst, W. A., Hettiarachchi, S. B., and N. H. Koedam, 2000, "Four Decade Vegetation Dynamics in Sri Lankan Mangroves As Detected from Sequential Aerial Photography: A Case Study in Galle," *Bulletin of Marine Science*, 67(2):741–759.

Davis, J. H., 1940, *The Ecology and Geologic Role of Mangroves in Florida*, Washington, DC: Carnegie Institute Publication no. 517.

Definiens, 2004, *eCognition 2004. User Guide 4.0*, Munich, Germany, Definiens, 486 p.

Desclée, B., Bogaert, P., and P. Defourny, 2006, "Forest Change Detection by Statistical Object-Based Method," *Remote Sensing of Environment*, 102:1–11.

Dong, P., 2000, "Lacunarity for spatial heterogeneity measurement in GIS," *Geographic Information Sciences*, 6(1):20–26.

Giri, C. and J. P. Delsol, 1995, "Mangrove Forest Cover Mapping Using Remote Sensing Data in Conjunction with GIS," *Asian and Pacific Remote Sensing Journal*, 8(1).

Giri, C., Pengra, B., Zhu, Z., Singh, A., and L. L. Tieszen, 2007, "Monitoring Mangrove Forest Dynamics of the Sundarbans in Bangladesh and India Using Multitemporal Satellite Data from 1973 to 2000," *Estuarine, Coastal, and Shelf Science*, 73:91–100.

Green, E. P., Mumby, P. J., Edwards, A. J., Clark, C. D., and A. C. Ellis, 1998, "The Assessment of Mangrove Areas Using High Resolution Multispectral Airborne Imagery," *Journal of Coastal Research*, 425:433–443.

Held, A., Ticehurst, C., Lymburner, L., and N. Williams, 2003, "High Resolution Mapping of Tropical Mangrove Ecosystems Using Hyperspectral and Radar Remote Sensing," *International Journal of Remote Sensing,* 24:2739–2759.

Holmgren, P. K. and T. T. Thuresson, 1998, "Satellite Remote Sensing for Forestry Planning," *Journal of Forestry Research*, 13, 90–110.

IUCN, 2006, *Post-tsunami Mangrove Assessment: Species Composition Using Remote Sensing,* Bangkok, Thailand: World Conservation Union, Thailand Programme, Asia Regional Office, 100 p.

Ivits, E., and B. Koch, 2002, "Object-Oriented Remote Sensing Tools for Biodiversity Assessment: A European Approach," in Proceedings of the 22nd EARSeL Symposium, Prague, Czech Republic, 4–6 June 2002, Rotterdam, The Netherlands: Millpress Science Publishers.

Jensen, J. R., 2004, *Introductory Digital Image Processing. A Remote Sensing Perspective*, Upper Saddle River, NJ: Prentice Hall, 316 p.

Jusoff, K., 2006, "Individual Mangrove Species Identification and Mapping in Port Klang Using Airborne Hyperspectral Imaging," *Journal of Sustainability Science and Management*, 1(2):27–36.

Lillesand, T. M., Kiefer, R. W., and J. W. Chipman, 2004, *Remote Sensing and Image Interpretation*, 5th ed., New York, NY: John Wiley and Sons, 763 p.

Lu, D., and Q. Weng, 2007, "A Survey of Image Classification Methods and Techniques for Improving Classification Performance," *International Journal of Remote Sensing*, 28(5): 823–870.

Mandelbrot, B. B., 1983, *The Fractal Geometry of Nature*, New York,. NY: Freeman and Co.

Mandelbrot, B., 1995, "Measures of Fractal Lacunarity: Minkowski Content and Alternatives," *Progress in Probability*, 37:15–42.

McKee, K. L. 1995, "Seedling Recruitment Patterns in a Belizean Mangrove Forest: Effects of Establishment Ability and Physico-chemical Factors," *Oecologia*, 101:448–460.

Myint, S. W. and N. S. N Lam, 2005a, "A Study of Lacunarity-Based Texture Analysis Approaches to Improve Urban Image Classification," *Computers, Environment, and Urban Systems*," 29:501–523.

Myint, S. W., and N. S. N Lam, 2005b, "Examining Lacunarity Approaches in Comparison with Fractal and Spatial Autocorrelation Techniques for Urban Mapping," *Photogrammetric Engineering and Remote Sensing*, 71(8):927–937.

Myint, S. W., Mesev, V., and N. S. N Lam, 2006, "Texture Analysis and Classification through A Modified Lacunarity Analysis Based on Differential Box Counting Method," *Geographical Analysis*, 38:371–390.

Navulur, K, 2007, *Multispectral Image Analysis Using the Object-Oriented Paradigm*, Boca Raton, FL: CRC Press, Taylor and Frances Group, 165 p.

Rabinowitz, D., 1978, "Dispersal Properties of Mangrove Propagules," *Biotropica*, 10:47–57.

Ravan, S. A. and P. S. Roy, 1997, "Satellite Remote Sensing for Ecological Analysis of Forested Landscape," *Plant Ecology*, 131:129–141.

Smith, T. J., III, 1987, "Seed Predation in Relation to Tree Dominance and Distribution in Mangrove Forest," *Ecology*, 68:266–273.

Thom, B. G., 1967, "Mangrove Ecology and Deltaic Geomorphology: Tabasco, Mexico," *Journal of Ecology*, 55:301–343.

Townshend, J. R. G., 1981, *Terrain Analysis and Remote Sensing*, London, UK: George Allen and Unwin, 272 p.

Voss, R.., 1986, "Random fractals: Characterization and measurement," in *Scaling Phenomena in Disordered Systems*, Pynn, R. and A. Skjeltorp (Eds)., New York, NY: Plenum.

Wang, L., Sousa, W. P., and P. Gong, 2004a, "Integration of Object-Based and Pixel-Based Classification for Mapping Mangroves with IKONOS Imagery," *International Journal of Remote Sensing*," 25:5655–5668.

Wang, L., Sousa, W. P., Gong, P., and G. S. Biging, 2004b, "Comparison of IKONOS and QuickBird Images for Mapping Mangrove Species on the Caribbean Coast of Panama," *Remote Sensing of Environment*," 91:432–440.

Wang, L. and W. Sousa, 2007, "Distinguishing Mangrove Species with Laboratory Measurements of Hyperspectral Leaf Reflectance," *International Journal of Remote Sensing*, in press.

UNEP (United Nations Environment Programme), 2004, *Global Environment Outlook Yearbook 2004*, Nairobi, Kenya: UNEP [http://www.unep.org/geo/yearbook/yb2004/007.htm].